Solid State Communications 253 (2017) 6–9

Contents lists available at ScienceDirect

Solid State Communications

journal homepage: www.elsevier.com/locate/ssc

Communication

# Manipulable wave-vector filtering in a $\delta$-doped magnetic-barrier nanostructure

Yu Liu, Lan-Lan Zhang*, Mao-Wang Lu, Yong-Long Zhou, Fei Li

*Hunan First Normal University, Changsha 410205, China*

ARTICLE INFO

*Keywords:*
A. Magnetic-barrier nanostructure
A. The $\delta$-doping
D. Wave-vector filtering (WVF) effect
D. The WVF efficiency

ABSTRACT

We theoretically explore the control of the wave-vector filtering (WVF) effect in a realistic magnetic-barrier nanostructure with a $\delta$ -doping, which can be experimentally realized by depositing a ferromagnetic stripe on the top of a GaAs/Al$_x$Ga$_{1-x}$ As heterostructure. It is shown that an obvious WVF effect still exists when a $\delta$-doping is introduced into the device. It is also shown that the degree of the WVF effect can be controlled by tuning the weight and/or the position of the $\delta$-doping.

## 1. Introduction

For a modulation-doped semiconductor heterostructure, a high mobility two-dimensional electron gas (2EDG) is comprised in its interface. Moreover, confining the motion of the 2DEG in an inhomogeneous magnetic field at nanometer scale by means of the modern nanofabrication technique, e.g., depositing a nanosized ferromagnetic (FM) stripe on the surface of the GaAs/Al$_x$Ga$_{1-x}$ As heterostructure [1], can form the so-called magnetic nanostructure [2], such as the magnetic barrier or well and magnetic superlattice. In fact, such a kind of 2DEG nanostructures is the hybrid of the magnetic material and the semiconductor, where the former provides an inhomogeneous magnetic field influencing locally the motion of the electrons in the latter. Due to the small size, the low dimensionality and the particular magnetic confinement, the magnetic nanostructure possesses abundant quantum effects [3], e.g., the wave-vector filtering (WVF) effect [2,4], the electron-spin polarization [5,6] and the giant magnetoresistance (GMR) effect [7–9], which can be useful for exploiting new electronic devices [10].

With the progress of the modern materials growth techniques such as molecular beam epitaxy (MBE) and metal-organic chemical-vapor deposition (MOCVD), the dimensional control has approached the interatomic spacing, literally called the atomic layer doping [11]. Utilizing such a technique, a tunable $\delta$-potential can be precisely doped into the nanostructure for nanoelectronics applications, e.g., resonant tunneling devices with the $\delta$-doping have been realized in experiments [12,13]. More recently Lu et al. [14,15], applied the $\delta$-doping to manipulate the electron-spin filtering effect in realistic magnetic-barrier nanostructures. They found that the transmission, the conductance and the spin polarization depend strongly on the weight and/or the position of the $\delta$-doping. Thus, the spin filtering can be controlled expediently by adjusting the $\delta$-doping and the structurally-tunable spin filters can be achieved for spintronics applications. Several groups [16–22] confirmed Lu et al.'s findings by studying the modulation of the $\delta$-doping to the spin filtering in other magnetic nanostructures.

Very recently, the $\delta$-doping technique was further applied to control the GMR effect of the magnetic nanostructure for magnetoelectronics. Taking the $\delta$-function magnetic-barrier nanostructure into account Kong et al. [23], first studied the influence of the $\delta$-doping on the GMR effect. It is found that the magnetoresistance ratio is related closely to the weight and the position of the $\delta$-doping. And then, a manipulable GMR device based on the magnetic nanostructure was proposed successfully for magnetic information storage. Subsequently, the modulation of the $\delta$ -doping to the GMR effect in other magnetic nanostructures was investigated and corresponding structurally-controllable GMR devices were achieved successively [24–27]. Motivated by these brief reports, in the present work we explore the control of the $\delta$-doping to the wave-vector filtering (WVF) effect in the magnetic nanostructure and expect to obtain the manipulable wave-vector filter.

## 2. Model and theoretical method

We consider a realistic magnetic-barrier nanostructure, as is schematically shown in Fig. 1(a), which can be experimentally realized [28,29] by the deposition, on top of the GaAs/Al$_x$Ga$_{1-x}$ As heterostructure, of a FM stripe with an in-plane magnetization. The magnetized FM stripe will induce a magnetic field along the $z$-direction, which

* Corresponding author.
*E-mail address:* llzhang02@126.com (L.-L. Zhang).

http://dx.doi.org/10.1016/j.ssc.2017.01.016
Received 17 September 2016; Received in revised form 20 December 2016; Accepted 16 January 2017
Available online 24 January 2017
0038-1098/ 

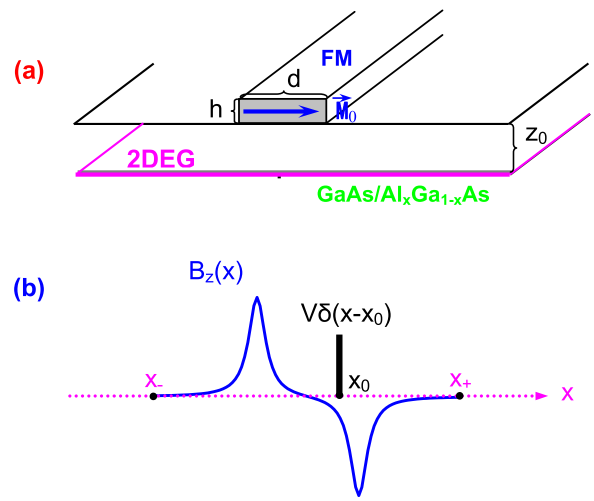


**Fig. 1.** (a) Schematic illustration of the magnetic-barrier nanostructure—one FM stripe is deposited on the top of the GaAs/$Al_xGa_{1-x}$ As heterostructure and (b) the magnetic-field profile, where a $\delta$-doping [$V\delta(x-x_0)$] is included.

acts perpendicularly on the 2DEG in $(x, y)$ plane, as [30].

$$\begin{cases} \overrightarrow{B} = B_z(x)\hat{e}_z, \\ B_z(x) = B_0\left[\dfrac{z_0 d}{(x+d/2)^2+z_0^2} - \dfrac{z_0 d}{(x-d/2)^2+z_0^2}\right], \end{cases} \tag{1}$$

where $B_0 = M_0 h/d$, as well as $\mathbf{M}_0$, $h$, $d$ and $z_0$ stand for the magnetization, thickness, width and vertical distance to 2DEG plane of the FM stripe, respectively. Correspondingly, the magnetic vector potential can be written, in Landau gauge, by [31].

$$\begin{cases} \overrightarrow{\mathbf{A}} = [0, A_y(x), 0] \\ A_y(x) = B_0 d\left[\tan^{-1}\left(\dfrac{x+d/2}{z_0}\right) - \tan^{-1}\left(\dfrac{x-d/2}{z_0}\right)\right]. \end{cases} \tag{2}$$

A $\delta$-doping, $V\delta(x-x_0)$, can be into the above system by the atomic layer doping technique,[11] as is shown in Fig. 1(b), where the left and right ends of the magnetic nanostructure are assumed to be located in $x_-$ and $x_+$, respectively. The Hamiltonian describing such a system, within the single particle, effective mass approximation, is [14,15].

$$H = \frac{p_x^2}{2m^*} + \frac{[p_y + eA_y(x)]^2}{2m^*} + \frac{em^* g^* \sigma\hbar}{4m_0}B_z(x) + V\delta(x-x_0), \tag{3}$$

where the $m^*$, $m_0$ and $\overrightarrow{p} = (p_x, p_y)$ are the effective mass, the free mass and the momentum of the electron, respectively. Notice that the third item in the above equation is the Zeeman coupling or called the spin-field interaction. It plays a minor role in determining electronic transport property for the GaAs material system, and thus will be omitted in this work [32].

Due to the translational invariance along the $y$ axis for the magnetic nanostructure, the solution of the stationary Schrödinger equation, $H\Psi(x, y) = E\Psi(x, y)$, can be expressed by $\Psi(x, y) = \psi(x)\exp(ik_y y)$, where the $k_y$ is the wave-vector component in $y$ direction. Thus, the wave function $\psi(x)$ complies with the following one-dimensional (1D) Schrödinger equation

$$\left\{\frac{d^2}{dx^2} + \frac{2m^*}{\hbar^2}[E - U_{eff}(x, k_y, V, x_0)\right\}\psi(x) = 0, \tag{4}$$

with the effective potential [33] for the electron in the magnetic nanostructure as

$$U_{eff}(x, k_y, V, x_0) = \frac{[\hbar k_y + eA_y(x)]^2}{2m^*} + V\delta(x-x_0). \tag{5}$$

Clearly, this potential depends not only on the longitudinal wave-vector $k_y$ and the magnetic configuration $B_z(x)$, but also on the $\delta$ -doping, $V\delta(x-x_0)$. Actually, it is the $\delta$-doping dependence of the $U_{eff}(x, k_y, V, x_0)$ that gives rise to the possibility to manipulate the WVF effect of the magnetic nanostructure.[14,15] However, the $U_{eff}(x, k_y, V, x_0)$ is very complicated within the region $[x_-, x_+]$ for the realistic magnetic-barrier nanostructure presented in Fig. 1(a), therefore, it is impossible to solve exactly Eq. (4). Here, we resort to the improved transfer-matrix method (ITMM) [34] to numerically settle the 1D Schrödinger equation. No loss of generality, in incident and outgoing regions of the system, the wave function can be assumed as $\psi_{left}(x) = \exp(ikx) + \gamma\exp(-ikx)$, $x < x_-$ and $\psi_{right}(x) = \tau\exp(ikx)$, $x > x_+$, respectively, where $k = \sqrt{2E - k_y^2}$ and $\gamma/\tau$ is reflection/transmission amplitude. Following Ref. 34, the transmission coefficient for the electron with the incident energy $E$ across the magnetic nanostructure can be obtained as

$$T(E, k_y, V, x_0) = |\tau|^2. \tag{6}$$

Once the transmission probability is obtained, the degree of the WVF effect can be characterized by the so-called wavevector filtering efficiency, which can be defined by differentiating the transmission coefficient over the wavevector for a fixed incident energy as

$$\eta = \frac{\partial T}{\partial k_y}. \tag{7}$$

## 3. Results and discussion

For convenience, we express all relevant quantities in the dimensionless form by means of the cyclotron frequency $\omega_c = eB_0/m^*$ and the magnetic length $\ell_B = \sqrt{\hbar/eB_0}$, e.g., $x \longrightarrow \ell_B x$ and $E \longrightarrow \hbar\omega_c E$. In our numerical calculation, we take the GaAs system as the material for the 2DEG, i.e., $m^*_{GaAs} = 0.067m_0$, $g^*_{GaAs} = 0.44$ and $n_{e(GaAs)} \approx 10^{11}\ \mathrm{cm}^{-2}$, which leads to the basic units $\ell_B = 57.5$ nm and $E_0 = \hbar\omega_c = 0.34$ meV for an estimated magnetic field $B_0 = 0.2$ T, and partial structural parameters are chosen as $d = 1.0$, $z_0 = 0.1$, $x_- = -1.5$ and $x_+ = 1.5$ for simplicity.

Previous investigations [4,30] demonstrated that the magnetic nanostructure in Fig. 1(a) possesses a considerable WVF effect. Does it still have such a quantum effect when a $\delta$-doping is introduced? First of all, Fig. 2(a) shows the transmission probability versus the incident energy for the electron with the wavevector $k_y = -1.0$ (solid curve), 0.0 (dashed curve) and 1.0 (dotted curve), where the $\delta$-doping is set to be $V = 2.0$ and $x_0 = 0.5$. From this figure, a great anisotropy with the wavevector can be seen apparently, due to an essentially 2E process[2] for the electron tunneling through a magnetic nanostructure. That is to say, there exists an obvious discrepancy of the transmission between different wavevectors. Therefore, a considerable WVF effect appears in the magnetic nanostructure even if a $\delta$-doping is included. In order to see the WVF effect more clearly, Fig. 2(b) directly plots the variation of the transmission coefficient with the wavevector for the incident energy $E = 3.0$ (solid curve), 6.0 (dashed curve) and 9.0 (dotted curve), where the $\delta$-doping is the same as in Fig. 2(a). We can observe from this figure that, the transmission coefficient ($T$) changes drastically with the wavevector ($k_y$) for a given incident energy ($E$). This means that a strong WVF effect still exists in the magnetic nanostructure with a $\delta$ -doping. Another observation is form this figure that, the WVF effect shows up a great dependence on the incident energy ($E$), because the $T$-$k_y$ curve is widened with the $E$ becoming large. The degree of the WVF effect or the wavevector filtering efficiency as the function of the wavevector is shown in Fig. 2(c) for the incident energy $E = 3.0$ (solid line), 6.0 (dashed line) and 9.0 (dotted line), where the $\delta$-doping is taken to be the same as in Figs. 2(a) and 2(b). Indeed, an evident WVF effect can be seen clearly, which can be explained from the fact that an essentially 2D process for the electron through a magnetic nanostructure is the $\delta$ -doping independent. Moreover, the wavevector filtering

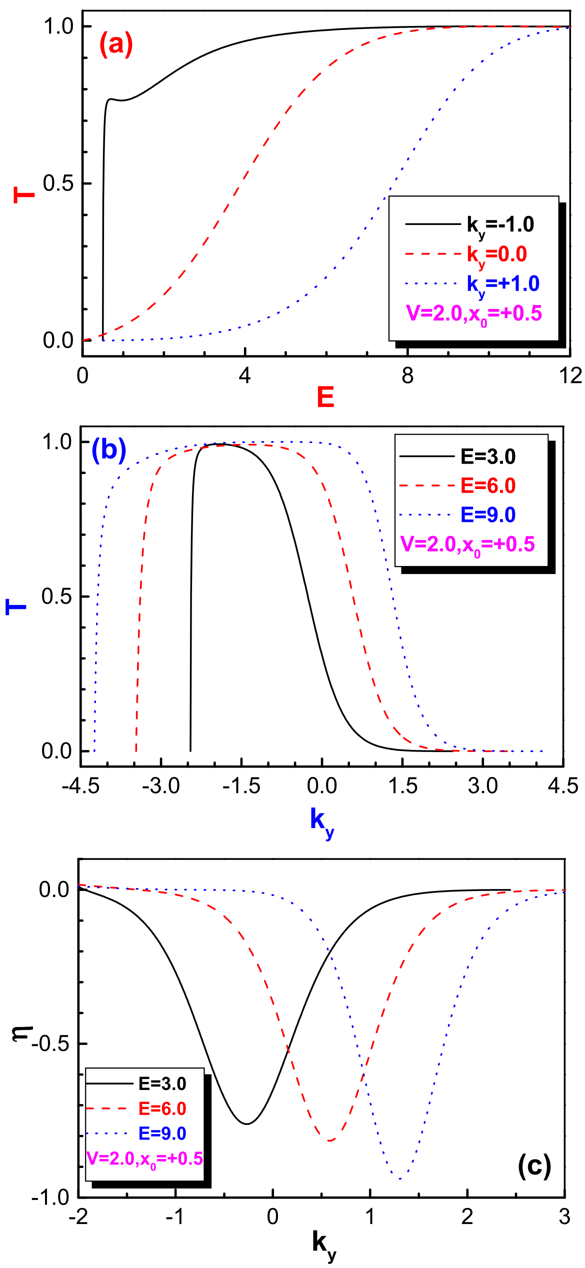


**Fig. 2.** The transmission probability as the functions of (a) the incident energy for the wavevector [$k_y = -1.0$ (solid curve), 0.0 (dashed curve) and +1.0 (dotted curve)] and (b) the wavevector for the incident energy [$E = 3.0$ (solid line), 6.0 (dashe line) and 9.0 (dotted line)], respectively, and (c) the WVF efficiency versus the wavevector for the incident energy [$E = 3.0$ (solid curve), 6.0 (dashed curve) and 9.0 (dotted curve)], where the $\delta$-doping is assumed to be $V = 2.0$ and $x_0 = +0.5$.

efficiency ($\eta$) exhibits a strong dependence on not only the wavevector ($k_y$) but also the incident energy ($E$), especially for the small incident angle and the high incident energy.

Having seen an appreciable WVF effect after a $\delta$-doping is introduced into the magnetic nanostructure, one wonder what impact such a doping has on the degree of the WVF effect (i.e., the wavevector filtering efficiency). Unquestionably, the $\delta$-doping will produce a significant influence on the WVF effect, since the effective potential ($U_{eff}$) of the magnetic nanostructure is related closely to the $\delta$-doping [see Eq. (5)]. In the following, we explore in detail how the weight ($V$) and the position ($x_0$) of the $\delta$-doping affect the degree of the WVF effect ($\eta$ ) of the magnetic nanostructure as shown in Fig. 1.

To begin with, we fix the position (such as $x_0 = +0.5$) and take the wavevector $k_y = 0.0$ (i.e., the normal incidence) as an example to investigate the effect of the weight ($V$) of the $\delta$-doping on the wavevector filtering efficiency. To this end, Fig. 3 plots the efficiency ($\eta$) versus the wavevector ($k_y$) for the weight of the $\delta$ -doping $V = 1.0$ (solid curve), 3.0 (dashed curve) and 5.0 (dotted curve), where the position of the $\delta$-doping remains unchanged at $x_0 = +0.5$ and the incident energy is taken as $E = 6.0$. The great difference of the wavevector filtering efficiency can be observed clearly for the different weight of the $\delta$-doping. With increasing the weight, the efficiency becomes small and the $\eta$-$k_y$ curve shifts upwards. In other words, the WVF effect in the magnetic nanostructure can be manipulated by properly adjusting the weight of the $\delta$-doping. The control of the wavevector filtering efficiency of the magnetic nanostructure via the weight of the $\delta$-doping can be seen more apparently from the inset of Fig. 3, where the efficiency ($\eta$) is directly calculated as the function of the weight ($V$) for the wavevector $k_y = 0.0$. The wavevector filtering efficiency varies dramatically with the weigh of the $\delta$-doping, especially within the range $5 > V > 0$. According to Eq. (5), the modulation of the weight ($V$) of the $\delta$-doping to the WVF effect originates clearly from the dependence of the effective potential ($U_{eff}$) on the weight ($V$).

Evidently, the $U_{eff}$ still depends on not only the weight ($V$) but also the position ($x_0$) of the $\delta$-doping. Therefore, the position ($x_0$) also will impact on the WVF effect of the magnetic nanostructure as shown in Fig. 1. Finally, in Fig. 4, we give the variation of the WVF efficiency ($\eta$) with the wavevector ($k_y$) for the position of the $\delta$-doping $x_0 = 0.0$ (solid line), 0.5 (dashed line) and 1.0 (dotted line), where the incident energy $E = 6.0$ are taken into account; while the weight of the $\delta$-doping is fixed

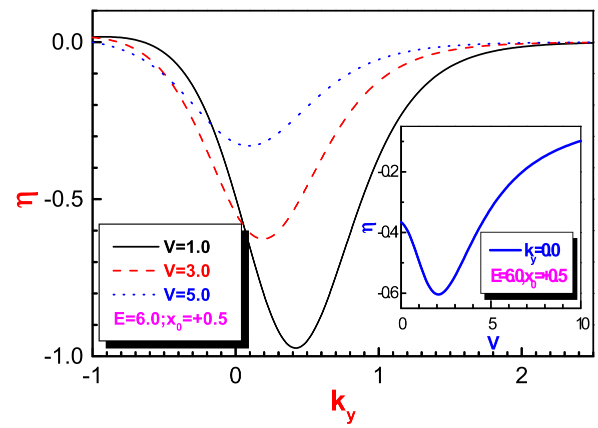


**Fig. 3.** The WVF efficiency ($\eta$) varies with the wavevector ($k_y$) for the weight of the $\delta$-doping $V = 1.0$ (solid line), 3.0 (dashed line) and 5.0 (dotted line), while in the inset the $\eta$ is plotted as the function of the weight of the $\delta$-doping for $E = 6.0$, where the position of the $\delta$-doping is fixed at $x_0 = +0.5$ and the wavevector is taken as $k_y = 0.0$.

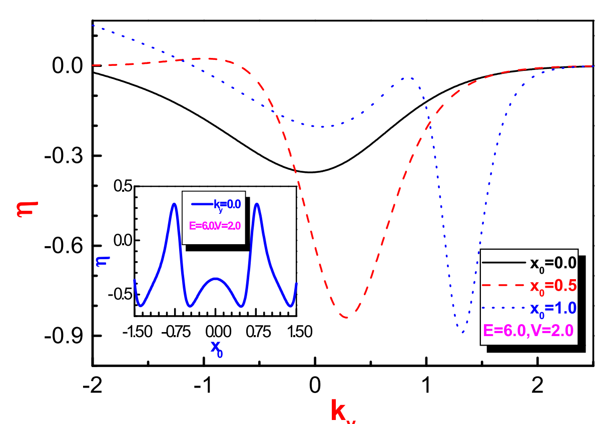


**Fig. 4.** For $E = 6.0$, the $\eta$ changes with the $k_y$ for the position of the $\delta$-doping $x_0 = 0.0$ (solid curve), 0.5 (dashed curve) and 1.0 (dotted curve), where the weight of the $\delta$-doping is taken as $V = 2.0$. The inset shows the $\eta$ as the function of the $x_0$ for the $E = 6.0$ and $k_y = 0.0$.

as $V = 2.0$. When the position of the $\delta$-doping changes, one can observe obviously from this figure the corresponding variation of the WVF efficiency. In particular, this change is more apparent if the $\delta$-doping deviates far from the centre of the magnetic nanostructure (cf. the dashed and dotted lines or the red and blue curves). This feature means that we also can manipulate expediently the WVF effect of the magnetic nanostructure (see Fig. 1) by changing the position of the $\delta$-doping. In order to observe more clearly this manipulation of the position, in the inset we directly plot the WVF efficiency ($\eta$) as the function of the position ($x_0$) of the $\delta$-doping, where the wavevector ($k_y$), the incident energy ($E$) and the weight ($V$) of the $\delta$-doping are the same as in Fig. 4. Indeed, the position of the $\delta$-doping has a strong control to the WVF effect in the magnetic nanostructure. Moreover, such a control to the WVF efficiency exhibits a symmetric behaviour with respect to the position of the $\delta$-doping, i.e., $\eta(-x_0) = \eta(x_0)$ for a given $E$ and a concrete $k_y$. This symmetric behaviour can be understood from the intrinsic symmetry [$B_z(-x) = -B_z(x)$ and $A_y(-x) = A_y(x)$] [35] and the fact that the transmission always is the identical for a particle tunneling through a potential barrier in the opposite directions.[36].

## 4. Conclusions

In summary, we have theoretically explored the control of a $\delta$-doping to the WVF effect in a magnetic-barrier nanostructure, which can be experimentally realized by depositing a ferromagnetic stripe with the horizontal magnetization on the top of the $GaAs/Al_x\,Ga_{1-x}$ As heterostructure and by using the atomic layer doping. It is confirmed that a sizeable WVF effect still exists even if a $\delta$-doping is included. It also is demonstrated that the WVF efficiency is strongly dependent on not only the weight but also the position of the $\delta$ -doping. These interesting findings will be helpful for designing structurally-controllable momentum filters for nanoelectronics applications.

## Acknowledgements

This work was supported by the National Natural Science Foundation of China (Grant No. 61464004).

## References

[1] H.A. Carmona, A.K. Geim, A. Nogaret, P.C. Main, T.J. Foster, M. Henini, S.P. Beaumont, M.G. Blamire, Phys. Rev. Lett. 74 (1995) 3009.
[2] A. Matulis, F.M. Peeters, P. Vasilopoulos, Phys. Rev. Lett. 72 (1994) 1518.
[3] A. Nogaret, J. Phys. Condens. Matter 22 (2010) 253210.
[4] M.W. Lu, L.D. Zhang, X.H. Yan, Nanotechnology 14 (2003) 609.
[5] Y. Guo, B.L. Gu, Z. Zeng, J.Z. Yu, Y. Kawazoe, Phys. Rev. B 62 (2000) 2635.
[6] G. Papp, P. Vasilopoulos, F.M. Peeters, 72, 2005. p.115315
[7] F. Zhai, Y. Guo, B.L. Gu, Phys. Rev. B 66 (2002) 125305.
[8] M.W. Lu, L.D. Zhang, J. Phys. Condens. Mat. 15 (2003) 1267.
[9] G. Papp, F.M. Peeters, J. Phys. Condens. Mat. 16 (2004) 8275.
[10] F.M. Peeters, X.Q. Li, Appl. Phys. Lett. 72 (1998) 572.
[11] F. Capasso, K. Mohammed, A.Y. Cho, R. Hull, A.L. Hutchinson, Appl. Phys. Lett. 47 (1985) 420.
[12] H.Q. Xu, Z. Shi, Phys. Rev. B 69 (2004) 237201.
[13] E.H. Ei Boudouti, B. Djafari-Rouhani, A. Akjouj, L. Dobrzynski, R. Kucharczyk, M. Steslicka, Phys. Rev. B 56 (1997) 9603.
[14] M.W. Lu, Z.Y. Wang, Y.L. Liang, Y.B. An, L.Q. Li, Appl. Phys. Lett. 102 (2013) 022410.
[15] M.W. Lu, Z.Y. Wang, Y.L. Liang, Y.B. An, L.Q. Li, EPL 101 (2013) 47001.
[16] J.D. Lu, Appl. Surf. Sci. 255 (2009) 7438.
[17] L.H. Shen, W.Y. Ma, G.L. Zhang, S.P. Yang, Physica E 71 (2015) 39.
[18] S. Li, M.W. Lu, Y.Q. Jiang, S.Y. Chen, AIP Adv. 4 (2014) 097112.
[19] J.D. Lu, Y.B. Li, S.J. Peng, H.Y. Liu, Y.H. Wang, H. Chen, Phys. Lett. A 380 (2016) 1668.
[20] H.Z. Xu, Y.F. Zhang, Appl. Phys. Lett. 84 (2004) 1995.
[21] L. Dell'Anna, A.De. Martino, Phys. Rev. B 80 (2009) 155416.
[22] W.Y. Ma, G.L. Zhang, S.Y. Chen, Y.Q. Jiang, S. Li, Phys. Lett. A 378 (2014) 1642.
[23] Y.H. Kong, S.Y. Chen, A.H. Li, X. Fu, Vacuum 122 (2015) 43.
[24] M.W. Lu, X.L. Cao, X.H. Huang, Y.Q. Jiang, S.P. Yang, Appl. Surf. Sci. 360 (2016) 989.
[25] L.H. Shen, G.L. Ma, D.C. Yang, Physica E 83 (2016) 450.
[26] L.L. Zhang, M.W. Lu, S.P. Yang, Q. Tang, Phys. Lett. A 380 (2016) 3520.
[27] Y.Q. Jiang, M.W. Lu, X.H. Huang, S.P. Yang, Q. Tang, J. Electr. Mater. 45 (2016) 4796.
[28] V. Kubrak, F. Rahman, B.L. Gallagher, P.C. Main, M. Henini, C.H. Marrows, M.A. Howson, Appl. Phys. Lett. 74 (1999) 2507.
[29] A. Nogaret, S.J. Bending, M. Henini, Phys. Rev. Lett. 84 (2000) 2231.
[30] J.Q. You, L.D. Zhang, P.K. Ghosh, Phys. Rev. B 52 (1995) 17243.
[31] F. Zhai, H.Q. Xu, Appl. Phys. Lett. 88 (2006) 032502.
[32] G. Papp, F.M. Peeters, Appl. Phys. Lett. 78 (2001) 2184.
[33] X.D. Yang, R.Z. Wang, Y. Guo, W. Yang, D.B. Yu, B. Wang, H. Yan, Phys. Rev. B 70 (2004) 115303.
[34] M.W. Lu, L.D. Zhang, X.H. Yan, Phys. Rev. B 66 (2002) 224412.
[35] F. Zhai, H.Q. Xu, Phys. Rev. Lett. 94 (2005) 246601;
F. Zhai, H.Q. Xu, Y. Guo, Phys. Rev. B 70 (2004) 085308.
[36] Y. Guo, H. Wang, B.L. Gu, Y. Kawazoe, Phys. Rev. B 61 (2000) 1728.